DOI: 10.1002/chem.200902072

Stereoselective Control by Face-to-Face Versus Edge-to-Face Aromatic Interactions: The Case of C_3-Ti^{IV} Amino Trialkolate Sulfoxidation Catalysts

Gabriella Santoni,[a] Miriam Mba,[a] Marcella Bonchio,[b] William A. Nugent,[c] Cristiano Zonta,*[a] and Giulia Licini*[a]

Dedicated to the Centenary of the Italian Chemical Society

Abstract: The stereoselective oxidation of differently functionalised benzyl phenyl sulfides has been examined by using enantiopure Ti^{IV} trialkanolamine complexes. These complexes efficiently catalyse the sulfoxidation with good stereoselectivities. The data highlight the contribution to the stereoselectivity of steric effects and non-covalent π–π interactions between the aromatic rings of the Ti^{IV} complex and those pertaining to the substrates. Enantiomeric excesses have been correlated with the electrostatic potential surfaces (EPS) of the reacting sulfides. The overall study leads to a mechanistic interpretation that explains the stereoselectivity of the system and dissects the role of aromatic and steric interactions in the stereoselective process.

Keywords: C_3 symmetry · catalytic oxidation · Pi interactions · stereoselectivity · sulfoxidation

Introduction

The experimental quantification of the role of intermolecular interactions has been a subject of intense research in recent years.[1] Molecular-recognition processes are intimately linked to many processes in chemistry and biology. Noncovalent interactions contribute significantly to the binding events of synthetic and natural systems, and they can be key elements in energies involved in the transitions states, therefore determining the reactivity of natural and artificial systems.[2] Among these, interactions between aromatic rings are judged to be responsible for many phenomena in chemical and biological sciences. As an example, they play an important role in the stabilization of molecules in solid and liquid-crystal phases.[3] In biological systems these have been identified as key factors in determining the structural and thus functional properties of nucleic acids and proteins.[4] Aromatic interactions have been investigated in a range of model systems.[5,6]

The possibility of using these interactions has also attracted scientists working in the field of stereoselective catalysis.[7] Indeed, interactions among aromatic groups have been shown to play a crucial role in some stereoselective reactions involving artificial catalysts. As an early example, Sharpless et al. reported on the influence of ligand–substrate π-stacking interactions in the asymmetric dihydroxylation of olefins.[8] Other important contributions have delineated the powerful role of aromatic ring interactions in controlling stereoselective reactions.[9] All of these results clearly indicate that the ligand–substrate aromatic interaction can generally reduce the conformational degrees of freedom and enhance the stereoselectivity in the selectivity-determining transition state. In some of these studies, a quantitative structure–reactivity relationship, involving the effect of the substitution in the aromatic rings, has been carried out. These studies have shown that the variation of the electronic density in the interacting aromatic rings can cause a change in stereoselectivity. This usually translates into a correlation between the observed stereoselectivities and the Hammett values of the aromatic substituents.

[a] Dr. G. Santoni, Dr. M. Mba, Dr. C. Zonta, Prof. G. Licini
Dipartimento Scienze Chimiche,
Università di Padova, via Marzolo 1, Padova (Italy)
Fax: (+39) 0498275239
E-mail: cristiano.zonta@unipd.it
giulia.licini@unipd.it

[b] Dr. M. Bonchio
ITM-CNR, via Marzolo 1
35131 Padova (Italy)

[c] W. A. Nugent
Vertex Pharmaceuticals, Inc.
130 Waverly Street, Cambridge, MA 02138 (USA)

Supporting information for this article is available on the WWW under http://dx.doi.org/10.1002/chem.200902072.

However, these approaches can lead to spurious results for two reasons: 1) the substituents are directly conjugated with the reactive site varying both the extent of the intermolecular interactions and the reactivity of the system[10] and 2) the variation of the electrostatic distribution of an aromatic ring can be responsible not only for the variation of the extent of the aromatic interaction, but it can also vary the orientation of the interacting aromatic rings. In fact, it is known that the electron density of the aromatic partners can force the interaction to be face-to-face (called also π-stacking) or edge-to-face (also referred as T-shaped or CH–π interactions).[5h]

Our investigation into aromatic interactions in catalysis grew from studies on the stereoselective sulfoxidation catalysed by C_3-symmetric enantiopure titanium(IV) amino trialkolates complexes **1** (Scheme 1).[11] In previous studies it

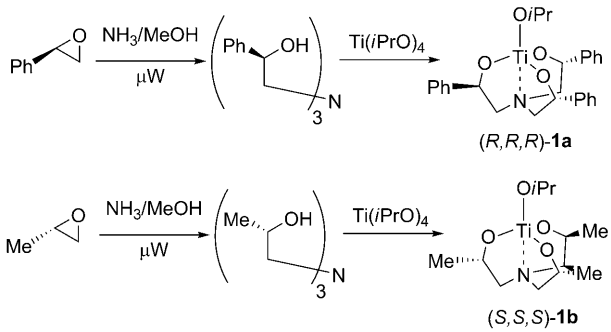

Scheme 1. Synthesis of the trialkanolamines and of the corresponding titanatranes (*R*,*R*,*R*)-**1a** and (*S*,*S*,*S*)-**1b**.[11f]

has been shown that trialkanolamines bind tightly to a titanium centre in a tetradentate fashion affording single, mononuclear C_3 complexes. These complexes furnish, upon addition of *tert*-butyl (TBHP) or cumyl hydroperoxide (CHP), the corresponding alkyl peroxo complexes, which are able to oxidize both secondary amines[12] and alkyl aryl sulfides, the latter in high enantiomeric excess (*ee*).[11b] These systems have also proven to be efficient when embedded in fluorinated polymeric membranes.[13]

In the quest for catalyst optimisation, it has been found that the nature of the ligand, substrate and alkyl peroxide are all relevant parameters, as far as reactivity and stereoselectivity are concerned. (*R*,*R*,*R*)-tri(1-phenylethanol)amine (**1a**) in conjunction with CHP provides the most reactive system also featuring the highest stereoselectivity. In particular, *ee* values up to 84% have been found in the sulfoxidation of benzyl phenyl sulfides favouring the *S* enantiomer with a sulfoxide/sulfone 77:23 ratio.[11b] Efficient stereoselective sulfoxidation of aryl benzyl sulfides has been reported with another Ti^{VI} catalyst, bearing (*S*,*S*)- or (*R*,*R*)-1,2-diphenyl-1,2-ethanediol as the ligand, with TBHP[14] and the Bolm catalyst ($VO(acac)_2$/Schiff base ligands/H_2O_2)[15] Furthermore, it was found that the enantiomeric excess of the products originated from two different and consecutive stereoselective processes: the asymmetric oxidation to sulfoxide and the kinetic resolution by oxidation to the sulfone. Both processes work in the same direction increasing the *ee* of the product as the reaction proceeds. In this early experiment, the pivotal role of the aromatic rings in the process was unambiguously proved.[11b] The replacement of an aromatic ring with an aliphatic chain, either in the complex, in the substrate or in the oxidant, resulted in a marked decrease in stereoselectivity. This prompted us to investigate in more detail the catalytic system, and in particular the role of aromatic interactions in the stereoselective process.

Herein we report a methodological study of the system in which it emerges that aromatic interactions, and in particular the subtle interplay between edge-to-face and face-to-face interactions, are responsible for the observed stereoselectivities. The analysis begins with a study of the effect of the aromatic moieties in the three partners of the reaction: catalyst, substrate and oxidant. This initial investigation is followed by a structure–reactivity relationship study on the effect of substitution of the aromatic ring of the substrate. The substitution in the aromatic ring has been designed to avoid conjugation between the substituent and the reactive sulfur centre, so that the resulting variation of *ee* values could be ascribed only to intermolecular interactions.

This study leads to: 1) the synthesis of a new series of sulfides and of the corresponding sulfoxides, 2) a quantitative structure–reactivity analysis able to explain the stereoselectivity of the reaction and 3) a dissection of the role of aromatic and steric interactions. The study is carried out by using a combined experimental and computational approach.

Results and Discussion

As noted above, the effect of the aromatic ring in the reaction partners was first investigated. In particular, the performances of catalysts, (*R*,*R*,*R*)-**1a** and the corresponding alkyl (*S*,*S*,*S*)-**1b** have been compared. The reactions involve the use of three different substrates bearing zero (methyl *n*-octyl sulfide **2**), one (methyl tolyl sulfide **3**) or two (benzyl tolyl sulfide **4b**) aromatic moieties, respectively, and two different oxidants: the "aliphatic" TBHP and the "aromatic" CHP (Scheme 2).

The experiments have been carried in the presence of a large excess of substrate to avoid the subsequent kinetic-resolution process of the sulfoxide leading to the formation of

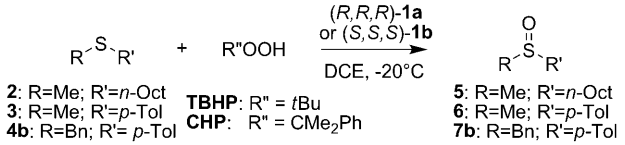

Scheme 2. Oxidation of sulfides (**2**, **3** and **4b**) catalysed by in situ formed (*R*,*R*,*R*)-**1a** or (*S*,*S*,*S*)-**1b** with CHP or TBHP (reaction conditions: $[\mathbf{2}\text{–}\mathbf{4}]_0 = 0.24$ M; sulfide/oxidant/catalyst 100:10:1; 1,2-dichloroethane (DCE); −20 °C.).

the sulfone. By using this protocol the pseudo-first order rate constants and stereoselectivities of the oxidation of sulfides **2**, **3** and **4b** to the corresponding sulfoxides **5**, **6** and **7b** have been determined (Figures 1 and 2).

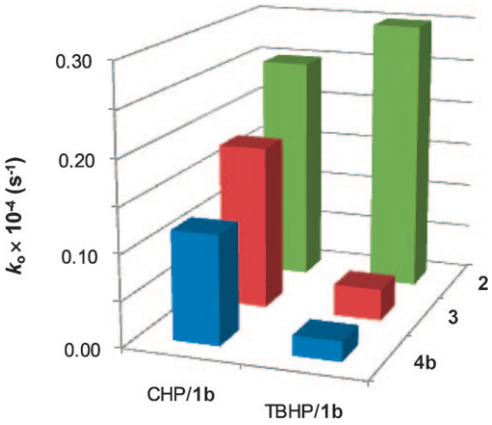

Figure 1. Pseudo-first-order rate constants for oxidation of sulfides (**2**, **3** and **4b**) catalysed by in situ formed (*S,S,S*)-**1b** with CHP or TBHP.

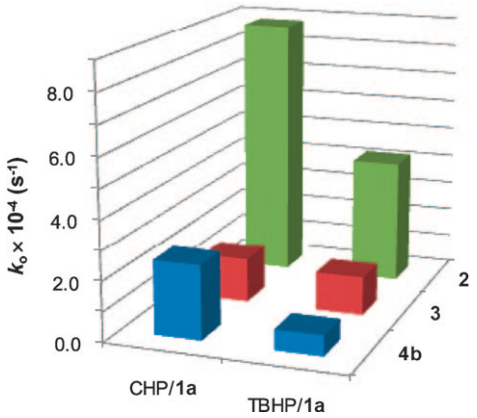

Figure 2. Pseudo-first-order kinetic constants for the oxidation of sulfides (**2**, **3** and **4b**) catalysed by in situ formed (*R,R,R*)-**1a** with CHP or TBHP.

The data confirm the better performance, in terms of stereoselectivity and reactivity, of catalyst (*R,R,R*)-**1a** relative to the fully aliphatic (*S,S,S*)-**1b**. The ligand effect on the sulfoxidation rate is likely explained by the more acidic character of the benzylic alcohol functions of (*R,R,R*)-**1a**, which results in a stronger Lewis acidity of the Ti^{IV} metal centre. Due to the electrophilic character of the oxygen-transfer process by the d^0 titanium–peroxo species, the expected relative reactivity of the sulfides should be **2**$\gg$**3**$>$**4b**, as a function of their nucleophilicity.[16] This is indeed what we found either with the aryl-free system **1b**/TBHP (see Table 1S, entries 1, 5 and 9 in the Supporting Information and Figure 1, data on the right) or when the aryl functionality is present just in the oxidant **1b**/CHP (Table 1S, entries 2, 6 and 10 and Figure 1, data on the left) or just in the catalyst **1a**/TBHP (Table 1S, entries 3, 7 and 11 and Figure 2, data on the right). Interestingly, a rather different behaviour is obtained when both the catalyst and the oxidant possess an aromatic group **1a**/CHP (Table 1S, entries 12 and 8 and Figure 2, data on the left). In this case the reactivity trend **2**$\gg$**4b**$>$**3** does not parallel the substrate nucleophilicity. In fact, benzyl tolyl sulfide **4b** reacts twice as fast as methyl *p*-tolyl sulfide **3**.

The important role of the aromatic system is also evident when examining the stereoselectivity of the process. By using the fully aromatic oxidizing system **1a**/CHP, very low *ee* values have been obtained with the fully aliphatic methyl *n*-octyl sulfide **2**. Moreover, the enantiomeric excess for the oxidation of benzyl *p*-tolyl sulfide **4b** is consistently higher, approximately double, that for methyl *p*-tolyl sulfoxide **3** (Figure 3). These data illustrate that stereoselectivity, and to some extent reactivity, strongly depend on the presence of aromatic groups in both reaction partners. This suggests a primary role for specific interactions among the π groups in the stereoselective step.

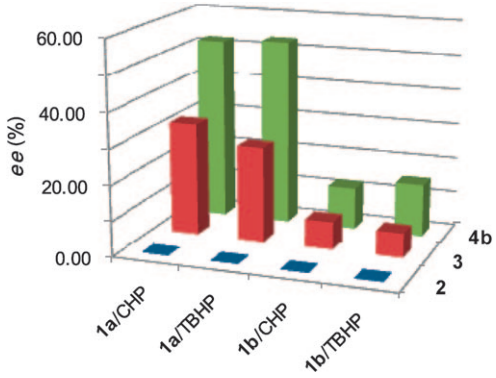

Figure 3. Enantiomeric excess for the oxidation of sulfides (**2**, **3** and **4b**) catalysed by in situ formed (*R,R*;*R*)-**1a** and (*S,S,S*)-**1b** with CHP or TBHP.

To discern the role of the aromatic units present in the catalytic system, differently substituted benzyl *p*-tolyl sulfides have been prepared. This family of sulfides has been chosen for two reasons. The first is the good stereoselectivity observed for the unsubstituted compound **4b**. The second is the opportunity to study substrates in which the substitution at the benzylic rings will have minimal impact on the reactivity of the sulfur atom.

Substituents in the benzyl systems have been chosen to vary the electronic and steric properties of the substrate. In particular, we synthesized compounds in which the aromatic rings have similar electrostatic characteristics with varying amounts of steric hindrance (**4a**–**e**), with halogens (**4h**–**j**), with strongly electron-withdrawing (**4k**–**n**) and electron-donating (**4f**–**g**) groups, a *meta,meta* disubstituted analogue (**4l**) and a sulfide containing a pentafluorophenyl ring (**4o**). The last system has been chosen because it is known to preferentially form face-to-face interactions with unsubstituted phenyl rings.[17]

Oxidations have been carried out by using the (*R,R,R*)-**1a**/CHP oxidizing system and slightly more concentrated

conditions than with the first experiments, ($[\mathbf{4a}–\mathbf{o}]_0 = 0.54$ M) and, as before, a tenfold excess of substrate has been used to avoid possible variation of *ee* values of the product due to kinetic resolution.[18] The *ee* values were determined before purification of the reaction mixture by using ^{1}H NMR spectroscopy in the presence of (*R*)-(−)-1-(9-anthryl)-2,2,2-trifluoroethanol as a chiral solvating agent (CSA) or via chiral HPLC. The absolute configuration (always *S*) has been assigned on the basis of the upfield shift in the ^{1}H NMR spectra of the diagnostic methyl protons of the *p*-tolyl group observed in the presence of the (*R*)-(−)-CSA or downfield shift when (*S*)-(+)-CSA has been used. The results are reported in Table 1.

The data highlight a marked variation in the stereoselectivities as a consequence of the variation of the benzyl aromatic ring. Yields up to > 99% have been obtained for all the reactions (and a distinct variation of the *ee* values has been observed from the highest excess of the 9-anthryl-substituted sulphide **7e** (*ee* = 71%) to the lowest represented by the pentafluorophenyl ring **7o** (*ee* = 45%). The impact of the electron-withdrawing/-donating capability of the substituents on the stereoselectivity of the reaction is immediately evident. For example, the comparison among the *p*-nitro (**4n**) and *p*-methoxy (**4g**)-substituted rings (Table 1, entries 7, and11) shows a significant difference in the *ee* values. On the other hand, aromatic groups with similar electronic features, such as benzene, naphthalene and anthracene (entries 1 and 3–5) also exhibit a large variation in *ee*. Thus both steric and electronic contributions must be considered in any model that seeks to rationalize these results.

To shed light on the nature and role of the intermolecular interactions between the catalyst and substrate in the transition state we investigated, by means of DFT calculations, the structure of the active peroxo complex. It is generally accepted that in the alkyl hydroperoxide activation by d^0 early transition metals, like Ti^{IV}, the active species is an η^2-coordinated alkyl peroxo complex (Scheme 3). Moreover,

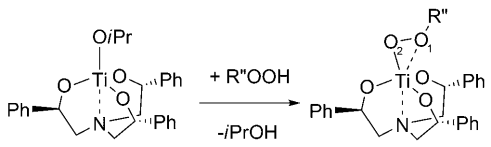

(*R*,*R*,*R*)-**1a** (*R*,*R*,*R*)-**8a**

Scheme 3. Formation of the Ti^{IV} η^2-alkyl peroxo complex **8a**.

the nucleophilic attack of the sulfide to the electrophilic peroxo oxygen (O_2) is along the antibonding σ* (O_1–O_2).[19]

This particular conformation of the alkyl peroxo–Ti^{IV} complex (*R*,*R*,*R*)-**8a** has been studied by the DFT method (B3LYP) by using the LANL2DZ basis set. In the minimised structure, the η^2 peroxo group occupies the upper axial position of the titanatrane structure, wherein the distances and angles are in line with previous studies (Table 2, Figure 4).[11d,20]

Table 1. Stereoselective oxidation of sulfides **5a**–**o** (0.54 M) catalysed by in situ formed (*R*,*R*,*R*)-**2b** (0.0054 M) with CHP (0.054 M) in DCE at −20 °C.[a]

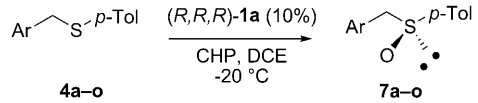

4a–o **7a–o**

	Ar	Yield [%][b]	*ee* [%][c]	log([*S*]/[*R*])	EPS [kJ mol^{-1}][d]
1	**a**	98	52	0.50	−84
2	**b**	89	54	0.52	−90
3	**c**	99	59	0.59	−66
4	**d**	82	51	0.49	−66
5	**e**	99	71	0.77	−54
6	Me_2N **f**	87	57	0.52	−116
7	MeO **g**	99	58	0.57	−92
8	F **h**	92	50	0.48	−56
9	Cl **i**	90	54	0.52	−46
10	Br **j**	99	60	0.60	−47
11	F_3C **k**	95	53	0.51	−36
12	NC **l**	92	49	0.47	−15
13	O_2N **m**	73	47	0.44	1
14	MeO, MeO **n**	99	52	0.50	−87
15	F, F, F, F, F **o**	72	45	0.42	73

[a] Reaction conditions: $[\mathbf{4a}–\mathbf{o}]_0 = 0.54$ M; sulfide/CHP/catalyst (*R*,*R*,*R*)-**1a** 100:10:1; DCE; −20 °C; reactions were carried out on a 5 mmol scale. [b] Isolated yield, based on oxidant. [c] Determined by ^{1}H NMR spectroscopy by using (−)-(*R*)-Pirkle's alcohol. [d] Calculated electrostatic surface potential by using the program package Spartan (EPS).

Table 2. Experimental and calculated distances of Ti^{IV}–η^2alkyl peroxo complexes.

Atoms[a]	X-ray[b]	RHF/3-21G(*)[c]	B3LYP/LANL2DZ[d]
Ti–O(1)	1.913	1.903	1.911
O(1)–O(2)	1.469	1.496	1.520
Ti–O(2)	2.269	2.117	2.300
Ti–N	2.299	2.397	2.416

[a] For oxygen labelling see Scheme 3. [b] See reference [20a]. [c] See reference [11d]. [d] The energy of the structure has been minimised by using Gaussian 03 software.[21]

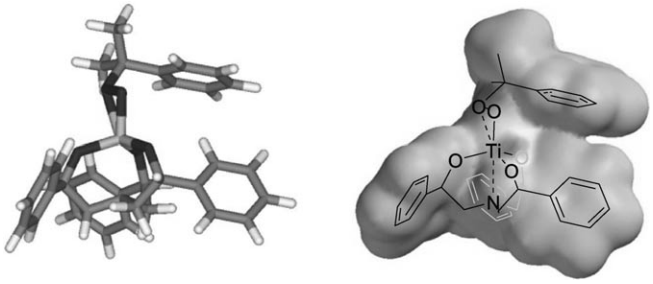

Figure 4. B3LYP/LANL2DZ-optimised structure of **8a** and calculated electrostatic potential surface.

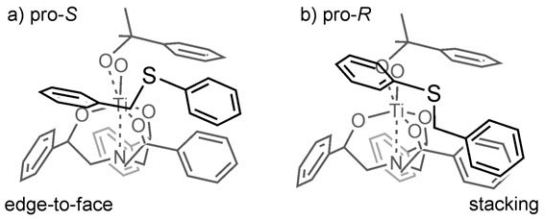

Scheme 4. Suggested mechanism for the nucleophilic attack of the substrate (along the σ* bond of the peroxo bond perpendicular to the plane of the paper). The two possible diasteromeric attacks for the sulphide are shown.

Among the possible conformations that the cumyl moiety can adopt, the more stable shows an edge-to-face interaction between the aromatic ring of the trialkanolamine ligand and the phenyl group of the cumyl hydroperoxide. In Figure 4, it is possible to observe the Van der Waals surface of the minimized structure of the reactive complex (*R,R,R*)-**8a**. The structure has been oriented to show the reactive trajectory of the nucleophilic attack of the substrate, above and perpendicular to the plane of the paper: in this stabilized conformation the peroxo–Ti^{IV} complex displays a structural pocket in which the aromatic interactions can play a primary role. Two possible approaches of the substrates, yielding the two enantiomeric sulfoxides, are dictated by the shape of the pocket and the directionality of the σ* bond of the reacting sulfide. As a consequence, two diastereomeric attacks can be envisaged (Scheme 4). If the sulfide is reacting with the pro-*S* lone pair its benzyl ring is interacting edge-to-face with the catalytic system **8a**. On the other hand, in the case of the pro-*R* lone-pair attack, the benzyl group is interacting face-to-face. From this observation, the preference for the pro-*S* attack indicates the tendency of the benzyl ring to participate in a stabilizing edge-to-face interaction or/and to avoid the face-to-face one. A confirmation of this assumption comes from the fact that the pentafluorophenyl **4o** (and to some extent also nitrobenzene **4m**), known to largely favour stacking interactions with unsubstituted phenyl rings, displays the lower *ee* values of all the series.

To extend the scope of this analysis to all the other substrates, we decided to consider the electrostatic properties of all the series of benzyl moieties. Since the present study utilizes mono- and polysubstituted aromatic rings in addition to the naphthyl, anthryl and pentafluorophenyl groups, the diverse cross-sections of aromatic rings could not be readily described by using the Hammett substituent constants, as shown in previous works on aromatic interactions.[5 h] Instead, calculated electrostatic potential surfaces (EPSs) seem more appropriate to generate a scale that describes the properties of the aromatic groups employed in this study.[1c] The calculated values of the EPSs at the centre of each of the aromatic groups are included in Table 1.

A plot of the experimental log([*S*]/[*R*]) against the ring centre EPSs of the aromatic moieties of the benzyl groups rules out any straightforward interpretation of the data (Figure 5a). However, a division of the aromatic systems into

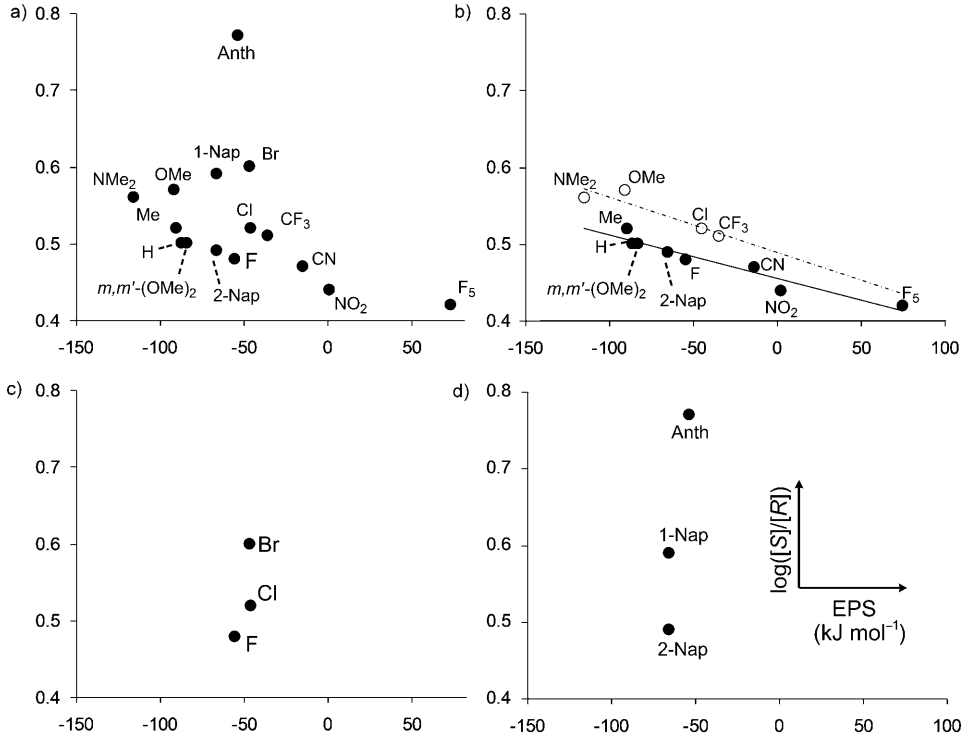

Figure 5. Plot of observed stereoselectivities expressed as log([*S*]/[*R*]) versus electrostatic potential surfaces EPS [kJ mol^{-1}] for: a) all the compounds, b) for compounds with substituents not hindered in *para* or *meta* positions (●,——: $R^2=0.93$) and with a hindered substituent in the *para* position (○,–•–•: $R^2=0.85$), c) for the halogen series and d) for the unsubstituted aromatic series.

three different classes gives prominence to the role of electrostatic and steric interactions. The contribution of the electrostatic factor is unambiguous if we focus our attention to eight sulfides **4a–c**,**h**,**l–o** with aromatic groups substituted by functions containing a steric hindrance, out of the ring plane, comparable to a phenyl ring (●,——: $R^2=0.93$) and with the four sulfides **4f**,**g**,**i**,**k** with a slightly more hindered substituent in the *para* position (○,–•–•: $R^2=0.85$) (Figure 5b). These plots extend across a wide electrostatic distribution with a good correlation. It covers rings from the pentafluorophenyl (**4o**) (lower stereoselectivity, *ee* = 45%), which is known to favour stacking interactions, to the dimethylamino-substituted ring (**4f**) known to favour the edge-to-face conformation (*ee* = 57%). This sequence suggests a defined and important role of electrostatics to the final stereoselection, revealing at the same time, an additive contribution of steric effects when a more hindered substituent is present in the *para* position (second correlation). This effect may be explained assuming a steric clash between the *para* substituent and the aromatic ring of the complex in the case of the pro-(*R*) attack. The presence of a disubstituted methoxy ring (**4l**) suggests that *meta* substituents do not interfere sterically with the outcome of the reaction.

The impact of the *para* steric factor is even more evident in the series of rings substituted in the *para* position with halogens (**4h–j** in Figure 5c). The three different halogens are known to have a similar influence on the electrostatic properties of the aromatic rings.[22] This is underlined by their similar EPSs. Among this series it is clear that the increasing steric size in the *para* position has an additive effect of the selectivity, favouring the formation of the *S* sulfoxides. The additive influence of the steric size on the stereoselectivity is also observed in the series constituted by polycondensed aromatic systems naphthyl and antryl (**4c–e** Figure 5d).

In this series, the increased dimensions of the aromatic systems (2-naphthyl **4d**, 1-naphthyl, **4c** and 9-anthryl **4e**) affords even larger differences in stereoselectivities, reaching the maximum value for the 9-anthryl derivative **4e**. (*ee* = 71%). Worthy of notice is the linear correlation that is obtained by plotting the experimental log([*S*]/[*R*]) values against the VDW radii of the halogens (F: 1.30, Cl: 1.75, Br: 1.95 Å) (■,——: $R^2=0.84$) and the width orthogonal to the C–C bond of the polycondensed aromatic ring, (2-naphthyl: 5.41, 1-naphthyl: 6.57, 9-anthryl: 8.99 Å) (◆,—— $R^2=0.99$; Figure 6), which indicates that the additive steric contribution of the benzyl moieties in the periphery can be also quantified, at least to a certain extent.

On the basis of the above analysis we suggest that the two diastereomeric approaches, yielding opposite enantiomers, are modulated by the occurrence of different intermolecular interactions between the aryl groups of the catalyst and the substrate. In particular, the favoured one, which affords the *S* sulfoxide, is characterised by a stabilizing edge-to-face interaction of the benzyl group with an aromatic ring of the catalyst (Scheme 4a). This approach is, therefore, more favoured by benzyl groups possessing electron-donating substituents In fact, edge-to-face interactions are favoured by electron-rich aromatic rings displaying negative EPS potentials. On the other hand it is not affected by the presence of substituents with higher steric hindrance. In the other approach, yielding the *R* enantiomer, the benzyl ring of the sulfide approaches the peroxo function forming a face-to-face interaction with one phenyl ring of the ligand (Scheme 4b). This interaction is eventually favoured by electron-withdrawing groups and, due to the presence of the cumyl ring, highly disfavoured by hindered aromatic rings. As the EPS of the benzyl ring becomes less negative, the stacking interaction becomes more favourable. For example, the pentafluorophenyl group **4o**, which has the most positive EPS and is known to give a face-to-face interaction, displays the lowest *ee*.

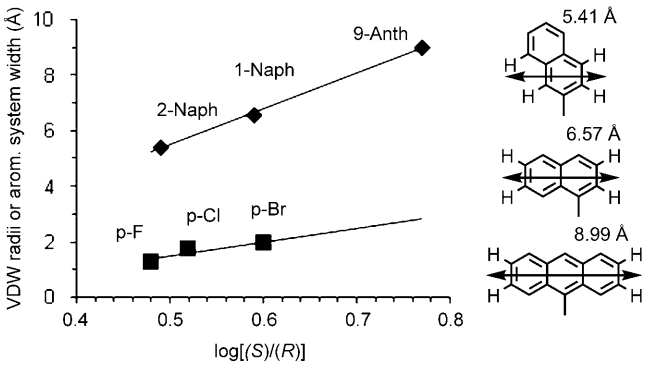

Figure 6. Plot of observed stereoselectivities expressed as log([*S*]/[*R*]) versus van der Waals radii or width of the polycondensed aromatic ring, orthogonal to the C–C bond [Å] for derivatives **4h–j** (F, Cl, Br) (■ ——: $R^2=0.84$), **4a** 2-naphtyl, **4c** 1-naphtyl and 9-anthryl **4e** (◆,——: $R^2=0.99$).

The contribution of the steric influences on the course of sulfoxidation is also evident. The highest *ee* values are obtained for molecules displaying hindered groups in *para* positions, as shown by the halogen series **4h–j** (F, Cl, Br), or when more hindered groups are present, as shown by the increasing *ee* values in the phenyl **4a**, 1-naphtyl **4c** and 9-anthryl **4e** series. These more hindered molecules are less prone to undergo the pro-(*R*) attack as a result of disfavoured stacking interactions as a consequence of steric repulsions with the cumyl aromatic ring.

Interestingly, what emerges from this analysis is that the selectivity of the process, that is, the discrimination between the diastereomeric transition states, obtained by only varying the electrostatic interactions of the aromatic partners is linear even if moderate. Indeed, comparing similar steric hindrances, the *ee* values observed for the most electron-poor substituent (pentafluoro **4o**) and the most electron-rich substituent (methoxy **4g**) only differ by 13%. This corresponds at −20°C to an energy difference of approximately 1 kJ mol^{-1}, in line with the experimental energies observed for π–π interactions. Much higher differences are observed for variation of the steric features of reacting partners with comparable EPSs and they linearly depend on the VDW radii of the halogen atoms in the *para* position or the dimen-

sions of the polycondensed aromatic systems. The reason why aromatic rings are important elements in the final stereoselectivity should be attributed to both effects, in which the steric features have a larger role than the electrostatic distribution.

Conclusion

The results observed in the oxidation of a series of benzyl tolyl sulfides with catalyst (*R,R,R*)-**1a** indicate that the origin of the substituent-dependent enantioselectivity in the oxygen-transfer reactions of sulfides is given by the competition of face-to-face and edge-to-face interactions between the ligand backbone and substrates, interactions occurring in the pheripheryof the systems involved in the reaction and not directly influencing the oxygen-transfer process. Even though these intermolecular interactions are weak, the direct contact reached between the aromatic rings of the reagent and of the ligand in the transition state is able to modulate the observed selectivity. The results also reveal that the stereoselective catalytic reaction provides a sensitive probe to investigate weak intermolecular interactions, such as π–π interactions and the additive steric contributions in transition states. The results provide useful information for understanding the influence of electronic and steric effects in catalysts possessing aromatic backbones or substituents on aromatic substrates and for the design of novel ligands.

Experimental Section

General methods: Chemicals and solvents were purchased from commercial suppliers and used as supplied. Sulfides **4a**, **4b**, **4g**, **4h** and **4i** were prepared as previously reported.[15] Complexes (*R,R,R*)-**1a** and (*S,S,S*)-**1b** were synthesized as previously reported.[11f] ^{1}H (250 MHz) and ^{13}C NMR (62.9 MHz) spectra were recorded with a Bruker AVANCE 250 spectrometer at 20 °C by using $CDCl_3$ as the solvent. Chemical shifts are given in ppm relative to TMS as the internal standard. Coupling constants (*J*) are reported in Hz. Chiral HPLC was performed by using a Lichrosorb S100, (*S,S*)-Dach DNB chiral column eluting with *n*-hexane/*i*-propanol 80:20. Specific rotations were recorded on a Perkin–Elmer 241 polarimeter at 25 °C in the solvents indicated. The sodium D line (589 nm) was used unless otherwise indicated. The units of α are 10^{-1} deg cm^2 g^{-1}. Enantiomeric excesses and absolute configurations were determined by ^{1}H NMR spectroscopy ($CDCl_3$, 250 MHz) in the presence of (*R*)-1-(9-anthryl)-2,2,2-trifluoroethanol or by chiral HPLC as indicated. Sulfoxides **7a**, **7b**, **7g**, **7h** and **7i** have been previously reported in an enantioenriched form.[21] Sulfoxide **7k** has been reported in racemic form only.[23]

Synthesis of thioethers: General procedure

Method A: Sodium (38.4 mmol) was dissolved in absolute ethanol (30 mL) under nitrogen at 0 °C. *p*-Thiocresol (32 mmol) was added to this solution followed by a solution of the corresponding benzyl chloride (32 mmol) in ethanol (100 mL). The mixture was stirred at RT until consumption of the starting materials was observed as judged by TLC or GCMS. Water (100 mL) was added, the layers were separated and the aqueous one was extracted with CH_2Cl_2 (3×75 mL). The combined organic layers were washed with NaOH 5% (1×150 mL) and brine (1×150 mL), dried on Na_2SO_4 and concentrated under reduced pressure. The product was purified by flash chromatography on silica gel.

Method B: DBU (16.6 mmol) and a solution of *p*-thiocresol (16.6 mmol) in acetonitrile (10 mL) were added in this order to a solution of the benzyl chloride (16.6 mmol) in acetonitrile (20 mL). The mixture was stirred at RT until consumption of the starting materials was observed as judged by TLC or GCMS. Water (30 mL) was added, the layers were separated and the aqueous one was extracted with CH_2Cl_2 (3×25 mL). The combined organic layers were washed with brine (1×50 mL), dried on Na_2SO_4 and concentrated under reduced pressure. The product was purified by flash chromatography on silica gel.

Method C: KOH (11.27 mmol) was added to a solution *p*-thiocresol (18.8 mmol) in absolute ethanol (60 mL). The mixture was heated at 80 °C and at this temperature a solution of the corresponding benzyl chloride (9.39 mmol) in ethanol (15 mL) was added. The mixture was refluxed for 2 h, then cooled to RT, quenched with water (50 mL) and concentrated. The residue was partitioned in water (50 mL) and $CHCl_3$ (40 mL). The layers were separated and the aqueous one was extracted with $CHCl_3$ (3×40 mL). The combined organic layers were washed with brine (1×90 mL), dried on Na_2SO_4 and concentrated under reduced pressure. The product was purified by flash chromatography on silica gel.

1-Naphthylmethyl *p*-tolyl sulfide (4c): Method C; orange oil; yield: 70%; ^{1}H NMR (250 MHz, $CDCl_3$): δ=8.17 (d, J=8.0 Hz, 1H), 7.99 (d, J=7.3 Hz, 1H), 7.78 (d, J=7.7 Hz, 1H), 7.61–7.49 (m, 2H), 7.38–7.24 (m, 4H), 7.10 (d, J=8.0 Hz, 2H), 4.54 (s, 2H), 2.35 ppm (s, 3H); ^{13}C NMR (62.9 MHz, $CDCl_3$): δ=136.72, 133.89, 133.02, 132.74, 131.39, 131.03, 129.60, 128.73, 128.12, 127.25, 126.14, 125.76, 125.20, 123.92, 37.88, 21.05 ppm; MS (70 eV): *m/z*: 115 (26), 141 (100), 264 (18) [M^+]; elemental analysis calcd (%) for $C_{18}H_{16}S$: C 81.77, H 6.10; found: C 81.42, H 6.07.

2-Naphthylmethyl *p*-tolyl sulfide (4d): Method A; white solid; yield: 89%; m.p. 94–96 °C; ^{1}H NMR (250 MHz, $CDCl_3$): δ=7.83–7.75 (m, 3H), 7.73 (s, 1H), 7.65–7.44 (m, 3H), 7.25 (d, J=8.0 Hz, 2H), 7.06 (d, J=8.0 Hz, 2H), 4.24 (s, 2H), 2.31 ppm (s, 3H); ^{13}C NMR (62.9 MHz, $CDCl_3$): δ=136.60, 135.17, 133.23, 132.49, 132.29, 130.79, 129.60, 128.18, 127.65, 127.60, 127.33, 127.01, 126.02, 125.70, 40.08, 21.01 ppm; MS (70 eV): *m/z*: 115 (23), 141 (100), 264 (20) [M^+]; elemental analysis calcd (%) for $C_{18}H_{16}S$: C 81.77, H 6.10; found: C 81.53, H 6.04.

9-Anthracenylmethyl *p*-tolyl sulfide (4e): Method A; yellow solid; yield: 60%; m.p. 124–128 °C; ^{1}H NMR (250 MHz, $CDCl_3$): δ=8.30 (s, 1H), 8.20 (d, J=8.4 Hz, 2H), 7.92 (d, J=8.0 Hz, 2H), 7.48–7.30 (m, 6H), 7.08 (d, J=7.8 Hz, 2H), 4.95 (s, 2H), 2.30 ppm (s, 3H); ^{13}C NMR (62.9 MHz, $CDCl_3$): δ=136.49, 133.55, 131.35, 130.29, 129.92, 129.65, 129.02, 127.78, 127.50, 126.05, 124.90, 124.03, 32.51, 21.01 ppm; MS (70 eV): *m/z*: 191 (100), 314 (10) [M^+]; elemental analysis calcd (%) for $C_{22}H_{18}S$: C 86.84, H 5.92; found: C 84.03, H 5.77.

(4-Dimethylaminobenzyl) *p*-tolyl sulfide (4f): Method B; white solid; yield: 73%; m.p. 85–87 °C; ^{1}H NMR (250 MHz, $CDCl_3$): δ=7.33 (d, J=8.0 Hz, 2H), 7.27 (d, J=8.8 Hz, 2H), 7.16 (d, J=8.0 Hz, 2H), 6.76 (d, J=8.8 Hz, 2H), 4.14 (s, 2H), 3.00 (s, 6H), 2.41 ppm (s, 3H); ^{13}C NMR (62.9 MHz, $CDCl_3$): δ=149.53, 135.80, 133.17, 129.96, 129.63, 129.45, 124.93, 112.40, 40.43, 38.97, 20.88 ppm; MS (70 eV): *m/z*: 118 (12), 134 (100), 257 (100) [M^+]; elemental analysis calcd (%) for $C_{16}H_{19}NS$: C 74.66, H 7.44, N 5.44; found: C 74.30, H 7.47, N 5.41.

4-Bromobenzyl *p*-tolyl sulfide (4j): Method A; white solid; yield: 86%; m.p. 73–76 °C; ^{1}H NMR (250 MHz, $CDCl_3$): δ=7.37 (d, J=8.4 Hz, 2H), 7.18 (d, J=8.0 Hz, 2H), 7.11–7.04 (m, 4H), 3.98 (s, 2H), 2.30 ppm (s, 3H); ^{13}C NMR (62.9 MHz, $CDCl_3$): δ=136.96, 136.94, 131.69, 131.46, 131.11, 130.46, 129.67, 120.88, 39.27, 21.28 ppm; MS (70 eV): *m/z*: 63 (13), 90 (30), 169 (100), 292 (2) [M^+], 294 (2) [M^++2]; elemental analysis calcd (%) for $C_{14}H_{13}BrS$: C 57.35, H 4.47; found: C 57.12, H 4.14.

***p*-Tolyl 4-trifluoromethyllbenzyl sulfide (4k)**: Method A; white solid; yield: 68%; m.p. 89–91 °C; ^{1}H NMR (250 MHz, $CDCl_3$): δ=7.51 (d, J=8.0 Hz, 2H), 7.33 (d, J=8.0 Hz, 2H), 7.19 (d, J=8.0 Hz, 2H), 7.07 (d, J=8.0 Hz, 2H), 4.06 (s, 2H), 2.31 ppm (s, 3H); ^{13}C NMR (62.9 MHz, $CDCl_3$) δ=142.12 (q, J=1.4 Hz), 137.16, 131.38, 131.24, 129.73, 129.05, 125.31 (q, J=3.8 Hz), 124.12 (q, J=271.9 Hz), 39.49, 21.04 ppm; MS (70 eV): *m/z*: 109 (17), 159 (100), 282 (53) [M^+]; elemental analysis calcd (%) for $C_{15}H_{13}F_3S$: C 63.82, H 4.64; found: C 63.54, H 4.66.

4-Cianobenzyl *p*-tolyl sulfide (4l): Method A; white solid; yield: 96%; m.p. 102–105°C; ^{1}H NMR (250 MHz, $CDCl_3$): δ=7.54 (d, J=8.0 Hz, 2H), 7.29 (d, J=8.0 Hz, 2H), 7.17 (d, J=8.0 Hz, 2H), 7.06 (d, J=8.0 Hz, 2H), 4.04 (s, 2H), 2.31 ppm (s, 3H); ^{13}C NMR (62.9 MHz, $CDCl_3$) δ= 143.69, 137.48, 132.13, 131.65, 130.73, 129.76, 129.45, 118.77, 110.74, 39.80, 21.04 ppm; MS (70 eV): m/z: 89 (17), 116 (100), 123 (19), 239 (56) [M^+], 240 (10) [M^++1]; elemental analysis calcd (%) for $C_{15}H_{13}NS$: C 75.27, H 5.47, N 5.86; found: C 74.98, H 4.49, N 5.83.

4-Nitrobenzyl *p*-tolyl sulfide (4m): Method A; yellow solid; yield: 96%; m.p. 102–105°C; ^{1}H NMR (250 MHz, $CDCl_3$): δ=7.07–7.37 (m, 8H), 4.09 (s, 2H), 2.32 ppm (s, 3H); ^{13}C NMR (62.9 MHz, $CDCl_3$): δ=145.86, 137.68, 131.87, 130.52, 129.84, 129.55, 128.21, 123.62, 39.62, 21.09 ppm; MS (70 eV): m/z: 78 (25), 90 (23), 123 (22), 136 (20), 213 (22), 259 (100) [M^+]; elemental analysis calcd (%) for $C_{14}H_{13}NO_2S$: C 64.84, H 5.05, N 5.40; found: C 64.80, H 5.02, N 5.38.

3,5-Dimethoxybenzyl *p*-tolyl sulfide (4n): Method A; white solid; yield: 89%; m.p. 92–94°C; ^{1}H NMR (250 MHz, $CDCl_3$): δ=7.23 (d, J=8.0 Hz, 2H), 7.07 (d, J=8.0 Hz, 2H), 6.42 (d, J=2.2 Hz, 2H), 6.33 (d, J=2.2 Hz, 2H), 4.00 (s, 2H), 3.74 (s, 6H), 2.31 ppm (s, 3H); ^{13}C NMR (62.9 MHz, $CDCl_3$): δ=160.66, 140.05, 136.56, 132.44, 130.68, 129.59, 106.64, 99.35, 55.26, 40.01, 21.01 ppm; MS (70 eV): m/z: 151 (100), 274 (36) [M^+]; elemental analysis calcd (%) for $C_{16}H_{18}O_2S$: C 70.04, H 6.61; found: C 70.51, H 6.59.

2,3,4,5,6-Pentafluorobenzyl *p*-tolyl sulfide (4o): Method A; white solid; yield: 83%; m.p. 64–66°C; ^{1}H NMR (250 MHz, $CDCl_3$): δ=7.28 (d, J= 7.7 Hz, 2H), 7.11 (d, J=7.7 Hz, 2H), 4.05 (s, 2H), 2.35 ppm (s, 3H); ^{13}C NMR (62.9 MHz, $CDCl_3$) δ=144.83 (dm, J=249.0), 140.23 (dm, J= 253.3), 138.53, 137.29 (dm, J=253.6 Hz), 133.19, 129.82, 112.63 (dt, J= 17.6, 4.0 Hz), 27.47, 21.05 ppm; MS (70 eV): m/z: 45 (20), 123 (58), 181 (100), 304 (66) [M^+]; elemental analysis calcd (%) for $C_{14}H_9F_5S$: C 55.26, H 2.98; found: C 54.98, H 2.93.

Asymmetric oxidation of sulfides: General procedure: A two-necked 25 mL flask was charged with the corresponding sulfide (5 mmol), catalyst (*R*,*R*,*R*)-**1a** (24 mg, 0.05 mmol) and dry 1,2-dichloroethane (6 mL) under nitrogen. The resulting solution was cooled to −20°C and a solution of CumOOH (95 mg, 0.5 mmol) in dry 1,2-dichloroethane (3.2 mL) was added. The mixture was stirred at −20°C until complete consumption of the oxidant (iodometric test). 5% Sodium metabisulfite (10 mL) was added and the mixture was stirred for 30 min at RT. The layers were separated and the aqueous one extracted with CH_2Cl_2 (3×10 mL). The combined organic layers were washed with 10% NaOH (1×30 mL) and brine (1×30 mL), dried on Na_2SO_4 and concentrated under reduce pressure. The product was purified by flash chromatography on silica gel.

Benzyl *p*-tolyl sulfoxide (7a): White solid; yield: 98%; 56% *ee* (*S*), determined by chiral HPLC; HPLC: t_R=11.1 (*S*), 16.8 min (*R*); $[\alpha]_D^{25}$=−143.2 (c=1.0 in acetone) (lit.[21] $[\alpha]_D^{20}$=−235.2 (c=0.7 in acetone) for 94% *ee*); all analytical data are in agreement with those previously reported.[21]

4-Methylbenzyl *p*-tolyl sulfoxide (7b): White solid; yield: 89%; 54% *ee* (*S*), determined by ^{1}H NMR spectroscopy ($CDCl_3$, 250 MHz) in the presence of (*R*)-1-(9-anthryl)-2,2,2-trifluoroethanol; $[\alpha]_D^{25}$=−110.1 (c=1.0 in dichloroethane) (lit.[21] $[\alpha]_D^{20}$=−43 (c=0.5 in chloroform) for >99% *ee*); all analytical data are in agreement with those previously reported.[15]

1-Naphthylmethyl *p*-tolyl sulfoxide (7c): White solid; yield: 99%; m.p. 156–159°C; 59% *ee* (*S*), determined by ^{1}H NMR spectroscopy in the presence of (*R*)-1-(9-anthryl)-2,2,2-trifluoroethanol; $[\alpha]_D^{25}$=−58.7 (c=1.0 in dichloromethane); ^{1}H NMR (250 MHz, $CDCl_3$): δ=8.01–7.98 (m, 1H), 7.87–7.78 (m, 2H), 7.52–7.49 (m, 2H), 7.33–7.14 (m, 5H), 7.02 (d, J= 7.0 Hz, 1H), 4.69 (AB, d, J=12.4 Hz, 1H), 4.33 (AB, d, J=12.4 Hz, 1H), 2.36 ppm (s, 3H); ^{13}C NMR (62.9 MHz, $CDCl_3$): δ=141.61, 139.95, 133.52, 131.81, 130.90, 129.55, 129.50, 129.40, 129.04, 128.65, 126.44, 125.84, 125.80, 125.07, 124.22, 123.33, 62.19, 21.30 ppm; MS (70 eV): m/z: 115 (25), 141 (100), 280 (2) [M^+]; elemental analysis calcd (%) for $C_{18}H_{16}OS$: C 77.11, H 5.75; found: C 76.86, H 5.80.

2-Naphthylmethyl *p*-tolyl sulfoxide (7d): White solid; yield: 82%; m.p. 164–167°C; 51% *ee* (*S*) determined by ^{1}H NMR spectroscopy in the presence of (*R*)-1-(9-anthryl)-2,2,2-trifluoroethanol; $[\alpha]_D^{25}$=−40.3 (c=1.0 in dichloromethane); ^{1}H NMR (250 MHz, $CDCl_3$): δ=7.83–7.71 (m, 3H), 7.49–7.46 (m, 3H), 7.31–7.19 (m, 4H), 7.10 (d, J=8.8 Hz, 1H), 4.26 (AB, d, J=12.4 Hz, 1H), 4.13 (AB, d, J=12.4 Hz, 1H), 2.39 ppm (s, 3H); ^{13}C NMR (62.9 MHz, $CDCl_3$): δ=141.65, 139.62, 133.07, 132.86, 130.89, 129.76, 129.57, 128.11, 127.83, 127.73, 127.63, 126.82, 126.26, 124.44, 64.07, 21.43 ppm; MS (70 eV): m/z: 115 (23), 141 (100), 280 (1) [M^+]; elemental analysis calcd (%) for $C_{18}H_{16}OS$: C 77.11, H 5.75; found: C 77.47, H 5.70.

9-Anthracenylmethyl *p*-tolyl sulfoxide (7e): White solid; yield: 99%; m.p. 142–145°C; 71% *ee* (*S*), determined by ^{1}H NMR spectroscopy in the presence of (*R*)-1-(9-anthryl)-2,2,2-trifluoroethanol; $[\alpha]_D^{25}$=−147.0 (c= 1.0 in dichloromethane); ^{1}H NMR (250 MHz, $CDCl_3$): δ=8.44 (s, 1H), 8.00–7.97 (m, 4H), 7.45–7.39 (m, 4H), 7.12 (d, J=8.3 Hz, 2H), 7.01 (d, J=8.3 Hz, 2H), 5.31 (AB, d, J=13.2 Hz, 1H), 4.96 (AB, d, J=13.2 Hz, 1H), 2.28 ppm (s, 3H); ^{13}C NMR (62.9 MHz, $CDCl_3$): δ=141.67, 139.81, 131.20, 131.07, 129.36, 129.06, 128.56, 126. 37, 124.99, 124.09, 123.79, 121.19, 57.63, 21.30 ppm; MS (70 eV): m/z: 191 (100), 330 (1) [M^+]; elemental analysis calcd (%) for $C_{22}H_{18}OS$: C 79.96, H 5.49; found: C 77.57, H 5.51.

4-Dimethylaminobenzyl *p*-tolyl sulfoxide (7f): White solid; yield: 87%; m.p. 123–125°C; 57% *ee* (*S*); $[\alpha]_D^{25}$=−120.1 (c=1.0 in dichloromethane); ^{1}H NMR (250 MHz, $CDCl_3$): δ=7.30 (d, J=8.3 Hz, 2H), 7.23 (d, J= 8.3 Hz, 2H), 6.85 (d, J=8.8 Hz, 2H), 6.59 (d, J=8.8 Hz, 2H), 4.05 (AB, d, J=12.6 Hz, 1H), 3.88 (AB, d, J=12.6 Hz, 1H), 2.93 (s, 6H), 2.40 ppm (s, 3H); ^{13}C NMR (62.9 MHz, $CDCl_3$): δ=150.33, 141.29, 131.55, 131.17, 129.44, 124.58, 116.36, 112.19, 63.55, 40.40, 21.44 ppm; MS (70 eV): m/z: 118 (15), 134 (100), 257 (10) [M^+−O]; elemental analysis calcd (%) for $C_{16}H_{19}NOS$: C 70.29, H 7.00, N 5.12, S 11.73; found: C 69.47, H 7.89, N 5.34,S 10.53.

4-Methoxybenzyl *p*-tolyl sulfoxide (7g): White solid; yield: 99%; 58% *ee* (*S*), determined by ^{1}H NMR spectroscopy in the presence of (*R*)-1-(9-anthryl)-2,2,2-trifluoroethanol; $[\alpha]_D^{25}$=−106.4 (c=1.0 in dichloromethane) (lit.[21] $[\alpha]_D^{20}$=−87 (c=0.2 in chloroform) for >99% *ee*); all analytical data are in agreement with those previously reported.[15]

4-Fluorobenzyl *p*-tolyl sulfoxide (7h): White solid; yield: 99%; 50% *ee* (*S*), determined by ^{1}H NMRspectroscopy ($CDCl_3$, 250 MHz) in the presence of (*R*)-1-(9-anthryl)-2,2,2-trifluoroethanol; $[\alpha]_D^{25}$=−118.4 (c=1.0 in dichloroethane) (lit.[21] $[\alpha]_D^{20}$=−109 (c=0.4 in chloroform) for 71% *ee*); all analytical data are in agreement with those previously reported.[15]

4-Chlorobenzyl *p*-tolyl sulfoxide (7i): White solid; yield: 90%; 54% *ee* (*S*), determined by ^{1}H NMR spectroscopy ($CDCl_3$, 250 MHz) in the presence of (*R*)-1-(9-anthryl)-2,2,2-trifluoroethanol; $[\alpha]_D^{25}$=−108.6 (c=1.0 in dichloroethane) (lit.[21] $[\alpha]_D^{20}$=−140 (c=0.5 in chloroform) for 98% *ee*); all analytical data are in agreement with those previously reported.[15]

4-Bromobenzyl *p*-tolyl sulfoxide (7j): White solid; yield: 99%; m.p. 155–159°C; 60% *ee* (*S*), determined by ^{1}H NMR spectroscopy ($CDCl_3$, 250 MHz) in the presence of (*R*)-1-(9-anthryl)-2,2,2-trifluoroethanol; $[\alpha]_D^{25}$=−123.0 (c=1.0 in dichloromethane); ^{1}H NMR (250 MHz, $CDCl_3$): δ=7.37 (d, J=8.4 Hz, 2H), 7.27–7.23 (m, 4H), 6.84 (d, J=8.4 Hz, 2H), 3.96 (s, 2H), 2.40 ppm (s, 3H); ^{13}C NMR (62.9 MHz, $CDCl_3$): δ=141.80, 139.25, 131.93, 131.48, 129.64, 128.08, 125.87, 124.36, 62.49, 21.43 ppm; MS (70 eV): m/z: 56 (30), 89 (21), 90 (26), 169 (100), 171 (99), 308 (1) [M^+], 310 (1) [M^++2]; elemental analysis calcd (%) for $C_{14}H_{13}BrOS$: C 54.38, H 4.24; found: C 54.50, H 4.25.

***p*-Tolyl 4-trifluoromethylbenzyl sulfoxide (7k)**: White solid; yield 95%; 53% *ee* (*S*), determined by ^{1}H NMR spectroscopy ($CDCl_3$, 250 MHz) in the presence of (*R*)-1-(9-anthryl)-2,2,2-trifluoroethanol; $[\alpha]_D^{25}$=−97.6 (c= 1.0 in dichloroethane); all analytical data are in agreement with those previously reported.[15]

4-Cianobenzyl *p*-tolyl sulfoxide (7l): White solid; yield: 92%; m.p. 180–184°C; 49% *ee* (*S*), determined by ^{1}H NMR spectroscopy ($CDCl_3$, 250 MHz) in the presence of (*R*)-1-(9-anthryl)-2,2,2-trifluoroethanol; $[\alpha]_D^{25}$=−129.0 (c=1.0 in dichloromethane); ^{1}H NMR (250 MHz, $CDCl_3$): δ=7.53 (d, J=8.3 Hz, 2H), 7.28–7.23 (m, 4H), 7.06 (d, J=8.3 Hz, 2H), 4.11 (AB, d, J=12.6 Hz, 1H), 3.96 (AB, d, J=12.6 Hz, 1H), 2.41 ppm (s, 3H); ^{13}C NMR (62.9 MHz, $CDCl_3$): δ=149.11, 148.59, 148.45, 136.94, 131.45, 131.10, 130.45, 129.66, 120.88, 39.27, 21.05 ppm; MS (70 eV): m/z: 89 (25), 116 (100), 139 (60), 255 (8) [M^+]; elemental analysis calcd (%) for $C_{15}H_{13}NOS$: C 70.56, H 5.13, N 5.49; found: C 70.37, H 5.15, N 5.46.

4-Nitrobenzyl *p*-tolyl sulfoxide (7m): White solid; yield: 73%; m.p. 162–166°C; 47% *ee* (*S*), determined by ^{1}H NMR spectroscopy ($CDCl_3$, 250 MHz) in the presence of (*R*)-1-(9-anthryl)-2,2,2-trifluoroethanol; $[\alpha]_D^{25} = -129.0$ (*c* = 1.0 in dichloromethane); ^{1}H NMR (250 MHz, $CDCl_3$): $\delta = 8.10$ (d, *J* = 8.8 Hz, 2H), 7.26 (brs, 4H), 7.11 (d, *J* = 8.8 Hz, 2H), 4.17 (AB, d, *J* = 12.8 Hz, 1H), 4.00 (AB, d, *J* = 12.8 Hz, 1H), 2.41 ppm (s, 3H); ^{13}C NMR (62.9 MHz, $CDCl_3$): $\delta = 147.59$, 142.11, 138.36, 136.28, 131.19, 129.76, 124.12, 123.22, 61.80, 21.40 ppm; MS (70 eV): *m*/*z*: 89 (25), 116 (100), 139 (60), 275 (8) [M^+]; elemental analysis calcd (%) for $C_{14}H_{13}NO_3S$: C 61.07, H 4.76, N 5.09; found: C 60.84, H 5.05, N 5.06.

3,5-Dimethoxybenzyl *p*-tolyl sulfoxide (7n): White solid; yield: 99%; m.p. 115–120°C; 52% *ee* (*S*), determined by ^{1}H NMR spectroscopy ($CDCl_3$, 250 MHz) in the presence of (*R*)-1-(9-anthryl)-2,2,2-trifluoroethanol; $[\alpha]_D^{25} = -115.0$ (*c* = 1.0 in dichloromethane); ^{1}H NMR (250 MHz, $CDCl_3$): $\delta = 7.34$ (d, *J* = 8.2 Hz, 2H), 7.28 (d, *J* = 8.2 Hz, 2H), 4.11 (m, 1H), 3.87 (m, 1H), 4.11 (AB, d, *J* = 12.4 Hz, 1H), 3.87 (AB, d, *J* = 12.4 Hz, 1H), 3.70 (6H, s), 2.41 ppm (s, 3H); ^{13}C NMR (62.9 MHz, $CDCl_3$): $\delta = 160.56$, 142.02, 141.61, 139.72, 131.43, 129.51, 128.31, 125.89, 124.46, 107.98, 100.58, 64.22, 55.20, 21.36 ppm; MS (70 eV): *m*/*z*: 151 (100), 152 (19), 290 (1) [M^+]; elemental analysis calcd (%) for $C_{16}H_{18}O_3S$: C 66.18, H 6.25; found: C 66.47, H 6.23, S 10.63.

2,3,4,5,6-Pentafluorobenzyl *p*-tolyl sulfoxide (7o): White solid; yield: 72%; m.p. 117–122°C; 45% *ee* (*S*), determined by ^{1}H NMR spectroscopy in the presence of (*R*)-1-(9-anthryl)-2,2,2-trifluoroethanol; $[\alpha]_D^{25} = -75.8$ (*c* = 1.0 in dichloromethane); ^{1}H NMR (250 MHz, $CDCl_3$): $\delta = 7.30$ (d, *J* = 8.0 Hz, 2H), 7.30 (d, *J* = 8.0 Hz, 2H), 4.16 (AB, d, *J* = 12.8 Hz, 1H), 4.08 (AB, d, *J* = 12.8 Hz, 1H), 2.42 ppm (s, 3H); ^{13}C NMR (62.9 MHz, $CDCl_3$) $\delta = 145.45$ (dm, *J* = 250.6 Hz), 142.60, 140.96 (dm, *J* = 255.71 Hz), 139.03, 137.30 (dm, *J* = 252.01 Hz), 50.18, 21.38 ppm; MS (70 eV): *m*/*z*: 45 (17), 78 (15), 181 (100), 304 (66), 320 (4) [M^+]; elemental analysis calcd (%) for $C_{14}H_9F_5OS$: C 52.50, H 2.83; found: C 52.09, H 2.85.

Acknowledgements

Financial support from MIUR, FIRB 2003 CAMERE-RBNE03JCR5 project, University of Padova, Assegni di Ricerca 2006 (M.M.) and COST ACTION D40 Innovative Catalysis—New Processes and Selectivities.

[1] a) C. A. Hunter, *Chem. Soc. Rev.* **1994**, *23*, 101–109; b) E. A. Meyer, R. K. Castellano, F. Diederich, *Angew. Chem.* **2003**, *115*, 1244–1287; *Angew. Chem. Int. Ed.* **2003**, *42*, 1210–1250; c) K. N. Houk, A. G. Leach, S. P. Kim, X. Y. Zhang, *Angew. Chem.* **2003**, *115*, 5020–5046; *Angew. Chem. Int. Ed.* **2003**, *42*, 4872–4897; d) C. A. Hunter, *Angew. Chem.* **2004**, *116*, 5424–5439; *Angew. Chem. Int. Ed.* **2004**, *43*, 5310–5324.

[2] a) C. A. Hunter, C. M. R. Low, J. G. Vinter, C. Zonta, *J. Am. Chem. Soc.* **2003**, *125*, 9936–9937; b) P. W. N. M. van Leeuwen *Supramolecular Catalysis*, Wiley-VCH, Weinheim, **2008**; c) T. S. Koblenz, J. Wassenaar, J. N. H. Reek, *Chem. Soc. Rev.* **2008**, *37*, 247–262.

[3] a) A. S. Shetty, J. Zhang, J. S. Moore, *J. Am. Chem. Soc.* **1996**, *118*, 1019–1027; b) G. W. Coates, A. R. Dunn, L. M. Henling, J. W. Ziller, E. B. Lobkovsky, R. H. Grubbs, *J. Am. Chem. Soc.* **1998**, *120*, 3641–3649.

[4] a) W. Saenger, Principles of Nucleic Acid Structures, Springer Verlag, New York, **1984**; b) S. K. Burley, G. A. Petsko, *Science* **1985**, *229*, 23–28; c) C. A. Hunter, J. Singh, J. M. Thornton, *J. Mol. Biol.* **1991**, *218*, 837–846; d) C. A. Hunter, *J. Mol. Biol.* **1993**, *230*, 1025–1054; e) O. F. Schall, G. W. Gokel, *J. Org. Chem.* **1996**, *61*, 1149–1458; f) T. L. Ho, P. Y. Liao, K. T. Wang, *J. Chem. Soc. Chem. Commun.* **1995**, 2437–2438; g) D. Ranganathan, V. Haridas, R. Gilardi, J. L. Karle, *J. Am. Chem. Soc.* **1998**, *120*, 10793–10800; h) F. Chelli, F. L. Gervasio, P. Procacci, V. Schettino, *J. Am. Chem. Soc.* **2002**, *124*, 6133–6143; i) D. D. Boehr, A. R. Farley, G. D. Wright, J. R. Cox, *Chem. Biol.* **2002**, *9*, 1209–1217; j) S. Aravinda, N. Shamala, C. Das, A. Sriranjini, I. L. Karle, P. Balaram, *J. Am. Chem. Soc.* **2003**, *125*, 5308–5315; k) O. Guvench, C. L. Brooks, *J. Am. Chem. Soc.* **2005**, *127*, 4668–4674; l) P. Chakrabarti, R. Bhattacharyya, *Prog. Biophys. Mol. Biol.* **2007**, *95*, 83–137.

[5] a) F. Cozzi, M. Cinquini, R. Annuziata, J. S. Siegel, *J. Am. Chem. Soc.* **1993**, *115*, 5330–5331; b) F. Cozzi, F. Ponzini, R. Annunziata, M. Cinquini, J. S. Siegel, *Angew. Chem.* **1995**, *107*, 1092–1094; *Angew. Chem. Int. Ed. Engl.* **1995**, *34*, 1019–1020; c) *The CH-Pi Interaction: Evidence, Nature and Consequences* Wiley, Chichester, **1998**; d) C. A. Hunter, K. R. Lawson, J. Perkins, C. J. Urch, *J. Chem. Soc. Perkin Trans. 2* **2001**, *5*, 651–669; e) G. Chessari, C. A. Hunter, C. M. R. Low, M. J. Packer, J. G. Vinter, C. Zonta, *Chem. Eur. J.* **2002**, *8*, 2860–2867; f) C. A: Hunter, C. M. R. Low, J. G. Vinter, C. Zonta, *J. Am. Chem. Soc.* **2003**, *125*, 9936–9937; g) F. Cozzi, R. Annunziata, M. Benaglia, M. Cinquini, L . Raimondi, K. K. Baldridge, J. S. Siegel, *Org. Biomol. Chem.* **2003**, *1*, 157–162; h) S. L. Cockroft, J. Perkins, C. Zonta, H. Adams, S. E. Spey, C. M. R. Low, J. G. Vinter, K. R. Lawson, C. J. Urch, C. A. Hunter, *Org. Biomol. Chem.* **2007**, *5*, 1062–1080; i) S. L. Cockroft, C. A. Hunter, *Chem. Soc. Rev.* **2007**, *36*, 172–188; j) R. Annunziata, M. Benaglia, F. Cozzi, A. Mazzanti, *Chem. Eur. J.* **2009**, *15*, 4373–4381.

[6] a) C. A. Hunter, K. R. Lawson, J. Perkins, C. J. Urch, *J. Chem. Soc. Perkin Trans. 2* **2001**, 651–669; b) M. L. Waters, *Curr. Opin. Chem. Biol.* **2002**, *6*, 736–741. 26; c) M. L. Waters, *Biopolymers* **2004**, *76*, 435–445.

[7] a) G. B. Jones, *Tetrahedron* **2001**, *57*, 7999–8016; b) M. Nishio, *Tetrahedron* **2005**, *61*, 6923–6950.

[8] Hc C. Kolb, P. G. Andersson, K. B. Sharpless, *J. Am. Chem. Soc.* **1994**, *116*, 1278–1291.

[9] a) R. W. Quan, Z. Li, E. N. Jacobsen, *J. Am. Chem. Soc.* **1996**, *118*, 8156–8157; b) A. V. Malkov, L. Dufková, L. Farrugia, P. Koèovský, *Angew. Chem.* **2003**, *115*, 3802–3805; *Angew. Chem. Int. Ed.* **2003**, *42*, 3674–3677; c) T. Kawabata, M. Nagato, K. Takasu, K. Fuji, *J. Am. Chem. Soc.* **1997**, *119*, 3169–3170; d) P. Brandt, P. Roth, P. G. Andresson, *J. Org. Chem.* **2004**, *69*, 4885–4890; e) L. Ma, P. Jiao, Q. Zhang, J. Xu, *Tetrahedron: Asymmetry* **2005**, *16*, 3718–3734; f) A. Bisai, V. K. Singh, *Org. Lett.* **2006**, *8*, 2405–2408; g) S. K. Ginotra, V. K. Singh, *Org. Biomol. Chem.* **2006**, *4*, 4370–4374; h) Y. El-aziz, A. Schmitzer, S. K. Collins, *Angew. Chem.* **2006**, *118*, 982–987; *Angew. Chem. Int. Ed.* **2006**, *45*, 968–973; i) J. L. García Ruano, J. Alemán, I. Alonso, A. Parra, V. Marcos, J. Aguirre, *Chem. Eur. J.* **2007**, *13*, 6179–6195; j) L. Ma, P. Jiao, Q. Zhang, D.-M. Ming, J. Xu, *Tetrahedron: Asymmetry* **2007**, *18*, 878–884; k) S. K. Collins, Y. El-Azizi, A. R. Schmitzer, *J. Org. Chem.* **2007**, *72*, 6397–6408; l) D. K. Friel, M. L. Snapper, A. H. Hoveyda, *J. Am. Chem. Soc.* **2008**, *130*, 9942–9951; m) G. Tárkáni, P. Királi, S. Varga, B. Vakulya, T. Soós, *Chem. Eur. J.* **2008**, *14*, 6078–6086.

[10] M. Palucki, N. S. Finney, P. J. Pospisil, M. L. Güler, T. Ishida, E. N. Jacobsen, *J. Am. Chem. Soc.* **1998**, *120*, 948–954.

[11] a) W. A. Nugent, R. L. Harlow, *J. Am. Chem. Soc.* **1994**, *116*, 6142–6148; b) Di Furia, G. Licini, G. Modena, R. Motterle, *J. Org. Chem.* **1996**, *61*, 5175–5177; c) M. Bonchio, G. Licini, G. Modena, S. Moro, O. Bortolini, P. Traldi, W. A. Nugent, *Chem. Commun.* **1997**, 869–870; d) M. Bonchio, S. Calloni, F. Di Furia, G. Licini, G. Modena, S. Moro, W. A. Nugent, *J. Am. Chem. Soc.* **1997**, *119*, 6935–6936; e) G. Licini, M. Bonchio, G. Modena, W. A. Nugent, *Pure Appl. Chem.* **1999**, *71*, 463.472; f) L. Favretto, W. A. Nugent, G. Licini, *Tetrahedron Lett.* **2002**, *43*, 2581–2584.

[12] M. Forcato, W. A. Nugent, G. Licini, *Tetrahedron Lett.* **2003**, *44*, 49–52.

[13] a) M. G. Buonomenna, E. Drioli, W. A. Nugent, L. J. Prins, P. Scrimin, G. Licini, *Tetrahedron Lett.* **2004**, *45*, 7515–7518; b) M. G. Buonomenna, E. Drioli, R. Bertoncello, L. Milanese, L. J. Prins, P. Scrimin, G. Licini, *J. Catal.* **2006**, *238*, 221–231.

[14] a) M. I. Donnoli, S. Superchi, C. Rosini, *J. Org. Chem.* **1998**, *63*. 9392–9395; b) M. A. M. Capozzi, C. Cardellicchio, F. Naso, V. Rosito, *J. Org. Chem.* **2002**, *67*, 7289–7294.

[15] P. Kelly, S. E. Lawrence, A. R. Maguire, *Eur. J. Org. Chem.* **2006**, 4500–4509.

[16] M. Bonchio, S. Campestrini, V. Conte, F. Di Furia, *Tetrahedron* **1995**, *51*, 12363–12372.
[17] J. H. Williams, J. K. Cockroft, A. N. Fitch, *Angew. Chem.* **1992**, *104*, 1666–1669; *Angew. Chem. Int. Ed. Engl.* **1992**, *31*, 1655–1657.
[18] Reaction carried out by using one equivalent of CHP results in the formation of the corresponding sulfone and consequent kinetic resolution. This results in higher *ee* values. See the Supporting Information.
[19] a) F. E. Kühn, A. M. Santos, P. W. Roesky, E. Herdtweck, W. Scherer, P. Gisdakis, I. V. Yudanov, C. Di Valentin, N. Rösch, *Chem. Eur. J.* **1999**, *5*, 3603–3615; b) I. V. Yudanov, P. Gisdakis, C. Di Valentin, N. Rosch, *Eur. J. Inorg Chem.* **1999**, *12*, 2135–2145; c) D. Balcells, F. Maseras, G. Ujaque, *J. Am. Chem. Soc.* **2005**, *127*, 3624–3634. d) D. Balcells, F. Maseras, A. Lledóse, *J. Org. Chem.* **2003**, *68*, 4265–4274; e) A. Sartorel, M. Carraro, A. Bagno, G. Scorrano, M. Bonchio, *J. Phys. Org. Chem.* **2008**, *21*, 596–602; f) S. Lovat, M. Mba, H. C. L. Abbenhuis, D. Vogt, C. Zonta, G. Licini, *Inorg. Chem.* **2009**, *48*, 4724–4728.
[20] G. Boche, K. Möbus, K. Harms, M. Marsch, *J. Am. Chem. Soc.* **1996**, *118*, 2770–2771.
[21] Gaussian 03, Revision B02, M. J. Frisch, G. W. Trucks, H. B. Schlegel, G. E. Scuseria, M. A. Robb, J. R. Cheeseman, J. A. Montgomery, Jr., T. Vreven Jr., K. N. Kudin, J. C. Burant, J. M. Millam, S. S. Iyengar, J. Tomasi, V. Barone, B. Mennucci, M. Cossi, G. Scalmani, N. Rega, G. A. Petersson, H. Nakatsuji, M. Hada, M. Ehara, K. Toyota, R. Fukuda, J. Hasegawa, M. Ishida, T. Nakajima, Y. Honda, O. Kitao, H. Nakai, M. Klene, X. Li, J. E. Knox, H. P. Hratchian, J. B. Cross, C. Adamo, J. Jaramillo, R. Gomperts, R. E. Stratmann, O. Yazyev, A. J. Austin, R. Cammi, C. Pomelli, J. W. Ochterski, P. Y. Ayala, K. Morokuma, G. A. Voth, P. Salvador, J. J. Dannenberg, V. G. Zakrzewski, S. Dapprich, A. D. Daniels, M. C. Strain, O. Farkas, D. K. Malick, A. D. Rabuck, K. Raghavachari, J. B. Foresman, J. V. Ortiz, Q. Cui, A. G. Baboul, S. Clifford, J. Cioslowski, B. B. Stefanov, G. Liu, A. Liashenko, P. Piskorz, I. Komaromi, R. L. Martin, D. J. Fox, T. Keith, M. A. Al-Laham, C. Y. Peng, A. Nanayakkara, M. Challacombe, P. M. W. Gill, B. Johnson, W. Chen, M. W. Wong, C. Gonzalez, J. A. Pople, Gaussian, Inc., Pittsburgh PA, **2003**.
[22] G. Chessari, C. A. Hunter, J. L. Jiminez Blanco, C. M. R. Low and J. G. Vinter, *NMR in Supramolecular Chemistry*, Ed. M. Pons, Kluwer, **1999**, 331–334.
[23] N. Rodriguez, A. Cuenca, C. Ramirez de Arellano, M. Medeo-Simn, D. Peine, G. Asensio, *J. Org. Chem.* **2004**, *69*, 8070–8076.

Received: July 24, 2009
Published online: November 10, 2009

